Oncogene (2011) 1–16

www.nature.com/onc

ORIGINAL ARTICLE

Recognition of CD146 as an ERM-binding protein offers novel mechanisms for melanoma cell migration

Y Luo[1,2,3], C Zheng[1,2,3], J Zhang[1,2], D Lu[1,2], J Zhuang[1,2], S Xing[1,2], J Feng[1,2], D Yang[1,2] and X Yan[1,2]

[1]*National Laboratory of Biomacromolecules, Institute of Biophysics, Chinese Academy of Sciences, Beijing, China and* [2]*Chinese Academy of Sciences—University of Tokyo Joint Laboratory of Structural Virology and Immunology, Institute of Biophysics, Chinese Academy of Sciences, Beijing, China*

Tumor cell migration is a well-orchestrated multistep process that drives cancer development and metastasis. Previous data indicated that CD146 expression correlates with malignant progression and metastatic potential of human melanoma cells. However, the exact molecular mechanism of how CD146 promotes melanoma cell migration still remains poorly understood. Here, we report that CD146 physically interacts with actin-linking ezrin–radixin–moesin (ERM) proteins and recruits ERM proteins to cell protrusions, promoting the formation and elongation of microvilli. Moreover, CD146-promoted melanoma cell migration is linked to RhoA activation and ERM phosphorylation. CD146 recruits Rho guanine nucleotide dissociation inhibitory factors 1 (RhoGDI1) through ERM proteins and thus sequesters RhoGDI1 from RhoA, which leads to upregulated RhoA activity and increased melanoma cell motility. CD146-activated RhoA also promotes further ERM phosphorylation and activation through Rho-phosphatidylinositol-4-phosphate-5-kinase-phosphatidylinositol 4,5-biphosphate pathway, which reinforces CD146/ERM association. Thus, our results provide a mechanistic basis to understand the role of CD146 in regulating human melanoma cell motility.

Oncogene advance online publication, 4 July 2011; doi:10.1038/onc.2011.244

Keywords: cell migration; CD146; ERM proteins; RhoA; RhoGDI1

Introduction

Associations of transmembrane proteins with the cell cytoskeleton through their cytoplasmic tails regulate cell adhesion, migration, invasion, cortical morphogenesis and other plasma membrane processes (Luna and Hitt, 1992; Raucher *et al*., 2000; McClatchey and Fehon, 2009). Among these adaptor proteins mediating such associations, the highly conserved ezrin–radixin–moesin (ERM) proteins are crucial components that provide a regulatable link between membrane-associated proteins and the cortical cytoskeleton, and also participate in signal transductions (Bretscher *et al*., 2002; McClatchey, 2003). ERM proteins bind to the plasma membrane receptors at their NH_2-terminal (NT) domains and to F-actin at their COOH-terminal (CT) domains (Bretscher *et al*., 1997; Tsukita and Yonemura, 1999). By inhibitory self-association through intra- or intermolecular head-to-tail interactions between the NT and CT domains, several active binding sites on ERM proteins are masked. The activation process, a conformational change of the protein structure, is tightly regulated by the phosphorylation of a conserved threonine residue in the CT domain of each ERM protein (Louvet-Vallee, 2000). This phosphorylation is an important step in ERM protein activation, which disrupts the intramolecular interaction. Subsequently, activated ERM proteins are translocated from the cytosol to the membrane-cytoskeleton interface. Moreover, binding of phosphatidylinositol 4,5-biphosphate (PIP_2) to the NT domain is a prerequisite for ERM proteins to be phosphorylated and activated (Bretscher *et al*., 2000; Gervais *et al*., 2008). Functionally, ERM proteins have been implicated in signifying specialized membrane domains, promoting cell cytoskeleton remodeling and Rho GTPase activation, and inducing signal transduction (Bretscher *et al*., 2000). Several studies have also provided evidence that ERM expressions correlated with cell polarization, cell–cell or cell–ECM communication, and tumor cell transformation, motility and metastasis (Bretscher *et al*., 2002; McClatchey, 2003).

GDP dissociation inhibitors (GDIs) are important regulators of Rho GTPase function, which is involved in cell movements (DerMardirossian and Bokoch, 2005; Dovas and Couchman, 2005). GDIs inhibit dissociation of GDP from Rho proteins, preventing their conversions to the active, GTP-bound forms that are translocated to the membrane. In addition, by interacting with the active, GTP-bound form of Rho GTPase, GDIs also inhibit GTP hydrolysis, blocking both intrinsic GTPase activity and interactions of Rho proteins with effector molecules (Olofsson, 1999). Therefore, GDIs modulate the cycling of Rho GTPases

Correspondence: Professor X Yan, National Laboratory of Biomacromolecules, Institute of Biophysics, Chinese Academy of Sciences, 15 Datun Road, Beijing 100101, China.
E-mail: yanxy@ibp.ac.cn
[3]These authors contributed equally to this work.
Received 1 November 2010; revised 19 April 2011; accepted 25 April 2011

between cytosol and membranes. Importantly, RhoGDI1 was found to associate with a protein complex containing ERM proteins and CD44, which might be important for cell cytoskeleton remodeling and cell motility (Hirao *et al*., 1996).

CD146, also known as MCAM, MUC18, A32 antigen and S-Endo-1, was initially identified as a melanoma marker (Johnson *et al*., 1993). It is an integral membrane glycoprotein and belongs to the immunoglobulin superfamily. Its ectodomain contains five immunoglobulin-like domains and its cytoplasmic tail contains potential protein kinase C recognition sites and PDZ binding sites (Guezguez *et al*., 2006), indicating possible involvements in cell signaling. Although the extracellular ligand for CD146 is still unidentified, several studies have validated its functions in mediating the transduction of outside–in signals (Ouhtit *et al*., 2009). Anfosso *et al*. (1998) found that CD146 cross-linking by a monoclonal antibody (mAb), named S-endo1, triggers the phosphorylation of FAK through association with Fyn. Moreover, our previous works revealed that CD146 mediates tumor secretion-induced p38/IκB kinase/nuclear factor-κB signaling cascade, which is pivotal in inducing endothelial cell activation, leading to tumor angiogenesis (Yan *et al*., 2003; Bu *et al*., 2006; Zheng *et al*., 2009). Nevertheless, fully understanding of CD146 signaling relies on the identifications of not only the ligand, but also intracellular binding partners and effectors.

Several lines of evidence suggested that CD146 expression is upregulated in various types of experimental and clinical tumors, including melanoma (Shih *et al*., 1994; Johnson *et al*., 1997), prostate cancer (Wu *et al*., 2001, 2004), epithelial ovarian cancer (Aldovini *et al*., 2006), non-small-cell lung cancer (Kristiansen *et al*., 2003) and mesothelioma (Bidlingmaier *et al*., 2009). More importantly, ectopic expression of CD146 in melanoma was found in a positive correlation with tumorigenic transformation and the development of metastatic potential in both mice models and clinical data (Luca *et al*., 1993; Li *et al*., 2002). However, the underlying molecular mechanism of how CD146 promotes melanoma cell migration has not been elucidated yet. We reason that identifying signaling molecules downstream of CD146 would provide mechanistic clues. In this study, we find that CD146 physically interacts with ERM proteins and then recruits RhoGDI1 through ERM proteins. By using two human melanoma cell lines with different CD146 levels, A375 ($CD146^{high}$) and SK-mel-28 ($CD146^{low}$), we show the potential roles of CD146/ERM complex in inducing RhoA activation, ERM phosphorylation and human melanoma cell migration.

Results

CD146 associates with moesin and actin cytoskeleton

To understand the mechanism of how CD146 regulates cell movements, we searched for potential CD146-associated proteins using immunoprecipitation and proteomic analysis. Both β-actin and moesin were co-precipitated with endogenous CD146 and identified in mass spectrometric analysis (Figure 1a). As moesin is a membrane–cytoskeleton linker protein belonging to the ERM (ezrin–radixin–moesin) protein family, these results indicated that CD146 might be linked to the actin filament through moesin.

The association of endogenous CD146 with moesin was then verified by co-immunoprecipitation in four melanoma cell lines, A375, SK-mel-28, Mel-624 and Mel-888^{CD146} (Figures 1b and c). To further confirm the specific interaction between CD146 and moesin, particularly the N-terminal domain of moesin (designated as NT domain or moesin-FERM), we transfected moesin or moesin-FERM-expressing plasmids into HEK293T cells stably expressing human CD146. As the original HEK293T cells do not express CD146, the reconstitution of CD146/moesin complex served as evidence for possibly direct interaction (Figure 1d). Furthermore, glutathione *S*-transferase (GST) pull-down assays showed that GST-CD146cyt, CD146 cytoplasmic domain fused with GST, was readily bound by His-tagged moesin-FERM, whereas neither GST nor GST-beads exhibited this property (Figure 1e), demonstrating a direct physical interaction between CD146 cytosolic tail and moesin NT domain. It is worth noting that ezrin and radixin, the other two ERM family members, were also found associated with CD146 in melanoma A375 cells (Supplementary Figure S1), demonstrating the common ability of ERM proteins to link CD146 with actin cytoskeleton.

Moesin Thr558 phosphorylation is required for CD146/moesin association

As only the phosphorylated ERM adopting the active conformation associates with the cytoplasmic tails of membrane proteins, we further studied the association between CD146 and p-ERM by confocal microscopy analysis. CD146 was found colocalized with p-ERM on the cell membrane and with actin filament at submembranous F-actin cytoskeleton (Figure 2a). These images supported that p-ERM proteins function as linkers between membrane protein CD146 and actin cytoskeleton.

We next asked whether the association of CD146 with moesin requires its CT domain phosphorylation by transfecting A375 cells with plasmids expressing various GFP-tagged moesin mutants (Figure 2b). The expression of various GFP-tagged moesin mutants was confirmed by western blot using anti-ERM 38/87 and anti-GFP antibody (Supplementary Figure S2). Wild-type (WT) moesin-GFP was preferentially localized at the peripheral membrane; however, the unphosphorylatable moesin mutant T558A was distributed diffusely in the cytoplasm rather than concentrated on the cell membrane. In marked contrast, mutant T558D, which constitutively adopts the active configuration, was exclusively accumulated at the cell membrane and intensively colocalized with membrane-bound CD146 (Figure 2b). The fluorescent signal of the NT domain fragment tagged with GFP was also detected at the membrane, similar to the constitutively active form of moesin. These data implied that Thr558 phosphorylation

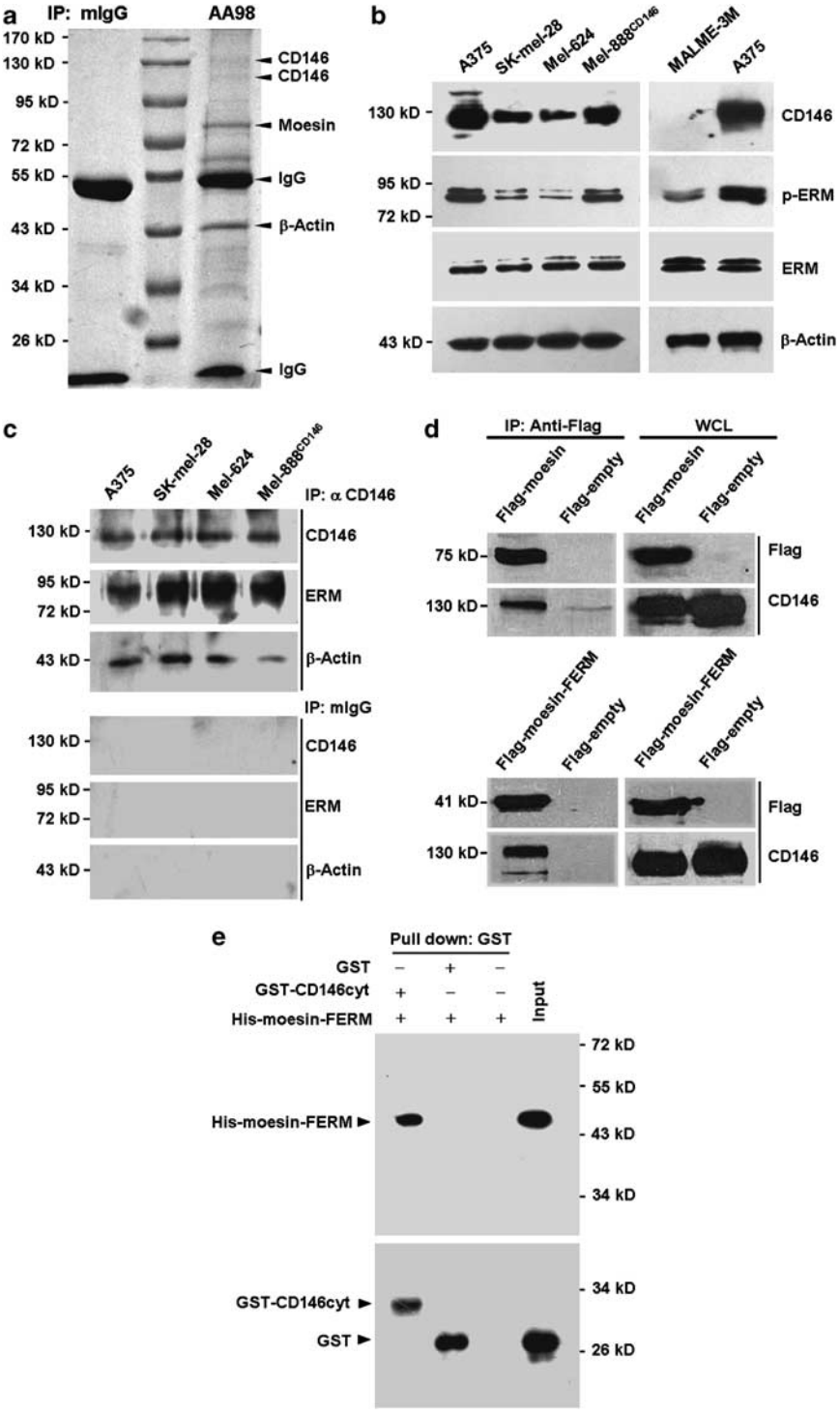

Figure 1 CD146 associates with moesin and actin cytoskeleton in human melanoma cells. (**a**) Co-immunoprecipitation (Co-IP) assays were performed using anti-CD146 mAb AA98. Protein bands were visualized by Coomassie blue staining. The proteins identified by mass spectrometry are indicated by arrowhead. Both the 130 and 110 kDa versions of CD146 proteins that have different glycosylation modifications were precipitated. (**b**) Expressions of CD146, p-ERM, ERM and β-actin proteins were detected in four human melanoma cell lines, A375, SK-mel-28, Mel-624 and Mel-888^{CD146}, by immunoblot. CD146-negative melanoma cell line MALME-3M served as a negative control. (**c**) Co-IP assays for association of endogenous CD146 with ERM and β-actin proteins in four human melanoma cell lysates. CD146 was precipitated by mAb AA98, and immunoblot was performed to analyze the immunoprecipitates. (**d**) Co-IP assays for association of CD146 with moesin and moesin-FERM in CD146-expressing HEK293T cells. Cells were transfected with Flag-moesin or Flag-moesin-FERM. Proteins were precipitated by anti-Flag mAb M2, and examined by immunoblot using antibodies against CD146. (**e**) Direct interaction between CD146 cytoplasmic tail and moesin-FERM *in vitro*. Proteins were expressed in *E. coli* and subjected to GST pull-down assays. His-moesin-FERM and GST-CD146cyt proteins were detected by immunoblot using anti-His or anti-GST antibody. Purified His-moesin-FERM and GST-CD146cyt proteins were loaded as the input lane.

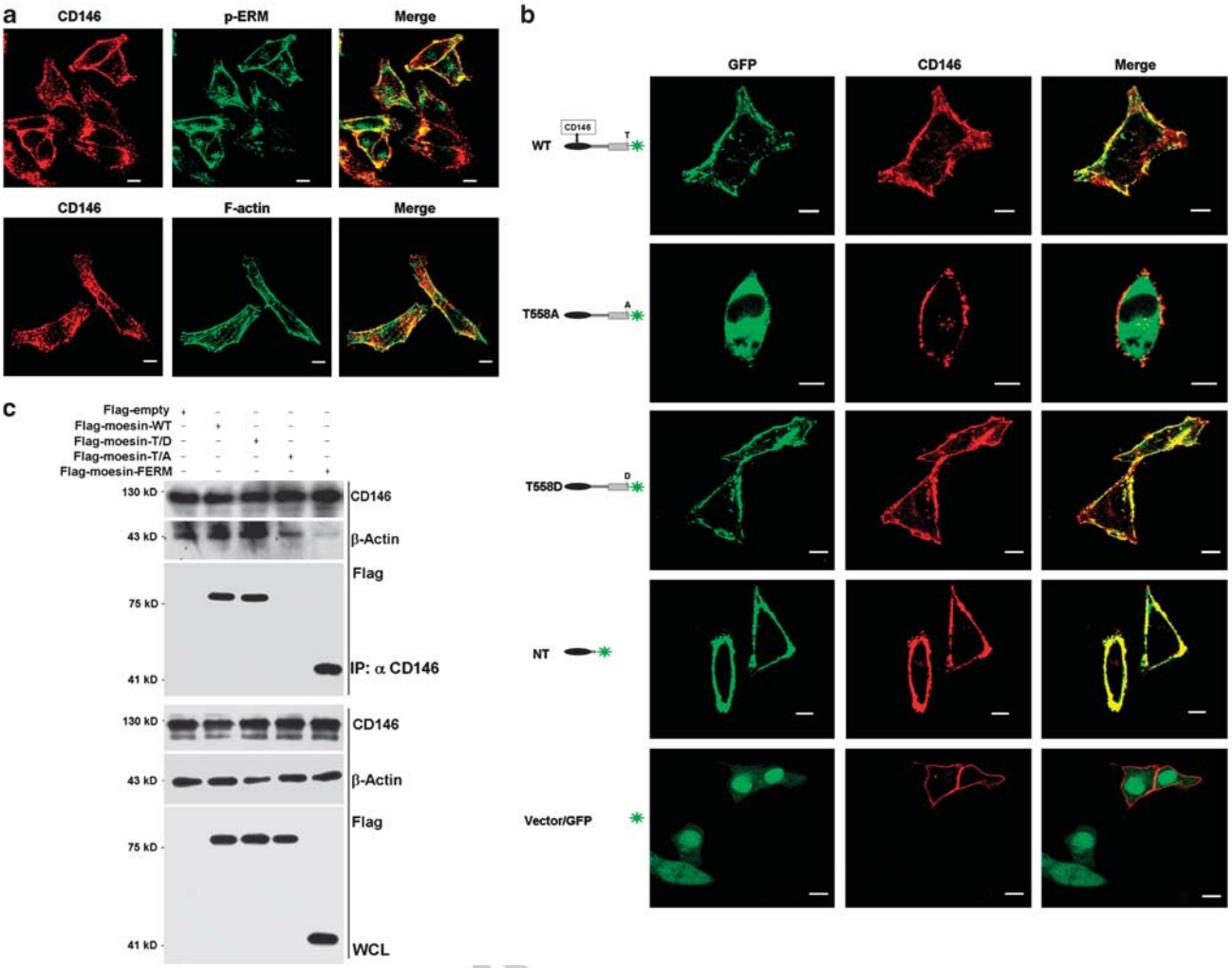

Figure 2 Moesin Thr558 phosphorylation is required for association with CD146. (**a**) Double-staining immunofluorescence and confocal microscopy analysis of CD146 colocalization with p-ERM (upper panel) and F-actin (lower panel) in A375 cells. Yellow is the overlapping of red (CD146) and green (p-ERM or F-actin) signals. Scale bar, 10 μm. (**b**) Left panel, GFP-tagged moesin constructs used in this study. Right panel, intracellular localization of moesin mutants in A375 cells. Transient transfectants were examined for the subcellular localization of various GFP-fused moesin mutants and CD146-RFP. (**c**) Interactions between CD146 and moesin mutants or actin cytoskeleton were detected by the immunoprecipitation using anti-CD146 mAb and immunoblot for Flag-tag and β-actin.

of moesin, which leads to the open conformation, could be indispensable for CD146/moesin association.

Biochemical analysis further confirmed the association of CD146 with moesin adopting active structures. Interactions between CD146 and WT, T558D or NT moesin were readily detected by co-immunoprecipitation, whereas interaction between CD146 and T558A moesin was undetectable (Figure 2c). *β*-Actin was strongly co-precipitated with CD146 only in WT and T558D moesin transfectants, but not in NT and T558A moesin transfectants. These findings demonstrated that Thr558 phosphorylation and the subsequent conformational changes of moesin are required for the bridging between actin filament and membrane CD146.

Positively charged KKGK motif is responsible for the firm interaction of CD146 with moesin

To further address the details of CD146/ERM interaction, we performed computational analyses and discovered a conserved positively charged amino-acid cluster KKGK motif in the juxtamembrane region of CD146 cytoplasmic tail, which might serve as a potential binding site for ERM proteins. To test this hypothesis, various CD146 mutants (Figure 3a) were co-expressed with WT moesin, respectively, in HEK293T cells and the reconstituted association between the two proteins was tested. Results showed almost equivalent moesin binding signal for WT CD146 and CD146-KKGKLP with Myc-tagged moesin, but only a faint signal for the CD146-ΔKKGK mutant (Figure 3b), which lacks the positively charged KKGK motif. Furthermore, ezrin and radixin also showed strong binding signals with WT CD146 and CD146-KKGKLP, but not CD146-ΔKKGK (Supplementary Figure S3), indicating that the juxtamembrane KKGK motif is required for the firm association of CD146 with ERM proteins.

Interestingly, in an *in vitro* binding assay, mAb AA14, which is raised against CD146 cytoplasmic domain and

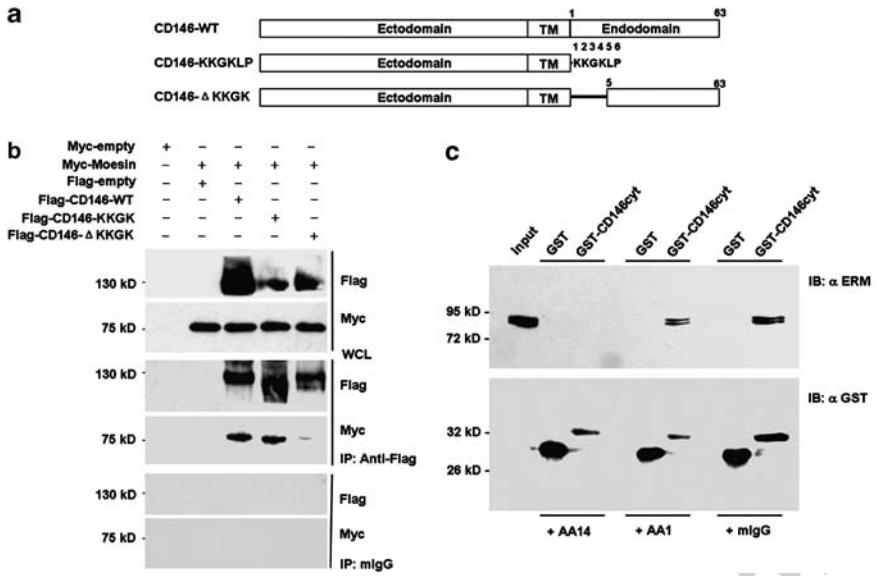

Figure 3 Positively charged KKGK motif is required for the firm interaction of CD146 with moesin. (**a**) A diagram illustrating the full-length WT and mutant CD146 proteins. TM, transmembrane region. (**b**) Positively charged KKGK motif is involved in the firm interaction of CD146 with moesin *in vivo*. HEK293T cells were co-transfected with constructs expressing Myc-moesin and Flag-CD146 or Flag-CD146-ΔKKGK or Flag-CD146-KKGKLP. Then, cell lysates were immunoprecipitated by anti-Flag mAb M2. Myc-moesin bound to CD146 variants was detected by immunoblot with anti-Myc mAb 9E10. (**c**) Effects of AA14 on the association of ERM proteins with the GST-CD146cyt beads. GST or GST-CD146cyt beads were incubated with A375 lysate in the presence of purified mAb AA14, AA1 or mouse immunoglobulin GG (100 μg/ml) for 60 min at 4 °C, followed by centrifugation and extensive washing. ERM proteins bound to GST-CD146cyt or GST were detected by immunoblot with anti-ERM mAb 38/87. Approximately 20 μl A375 cell lysate was loaded as the input lane. GST and GST-CD146cyt bound to the beads were detected by immunoblot with anti-GST antibody.

specifically recognizes the KKGK motif (Supplementary Figure S4), was capable of significantly suppressing the binding of recombinant GST-CD146cyt to ERM proteins (Figure 3c). In contrast, both anti-CD146 mAb AA1 that does not recognize the KKGK motif and the normal mouse immunoglobulin G did not affect the binding of CD146 to moesin. These data further supported that the KKGK motif within CD146 juxtamembrane region is indispensable for forming CD146/moesin complex.

Functional moesin is required for CD146-induced melanoma cell migration

As moesin is thought to be important for actin cytoskeleton rearrangement (Niggli and Rossy, 2008), we then tested the role of moesin in melanoma cell migration. It was found that the constitutively active moesin T558D mutant enhanced the transmigration of melanoma A375 (Figure 4a) and SK-mel-28 (Figure 4b) cells, whereas ectopic expression of T558A moesin led to a decrease of cell motility. However, overexpression of WT moesin had little effect on it, suggesting that the activation or phosphorylation of moesin rather than its protein level is mainly responsible for the increased cell motility. Moreover, cells expressing NT moesin showed remarkably diminished migration, indicating that the N-terminal domain alone acts in a dominant-negative manner to inhibit the endogenous ERM proteins by competing for the binding of membrane proteins. These results obtained in melanoma cells are consistent with previous observations for the functions of moesin in mediating cytoskeleton rearrangement and modulating cell migrations (Lee *et al*., 2004).

It has been previously found that CD146 could significantly promote human melanoma cell migration (Shih *et al*., 1994; Johnson *et al*., 1997). Therefore, we next assessed whether moesin is the downstream effector responsible for CD146-induced cell motility enhancement. In the presence of dominant-negative moesin mutant, moesin-FERM or moesin-T558A, neither CD146 overexpression nor CD146 knockdown could affect A375 cell migration any longer (Figures 4c and d, expressions were confirmed by western blot in Supplementary Figure S5). Same results were obtained in SK-mel-28 cells (Supplementary Figure S6). These data suggested that moesin is indispensible for CD146-promoted melanoma cell migration. More interestingly, knockdown of CD146 blocked the ability of constitutively active moesin T558D to drive cell migration (Figure 4e), indicating that the function of moesin also heavily relies on the presence of CD146. This result hinted that CD146 might be an essential membrane protein responsible for recruiting ERM and cytoskeleton during cell migration in melanoma.

As the formation of microvilli-like membrane protrusions is a very important characteristic for migrating cells (Crepaldi *et al*., 1997; Barreiro *et al*., 2004), we then tested the localizations of CD146 and ERM proteins on the microvilli-like minute projections of A375 cells. Interestingly, laser scanning confocal microscopy analysis showed a nearly perfect colocalization of CD146-RFP with moesin-GFP on A375 microvilli displayed in

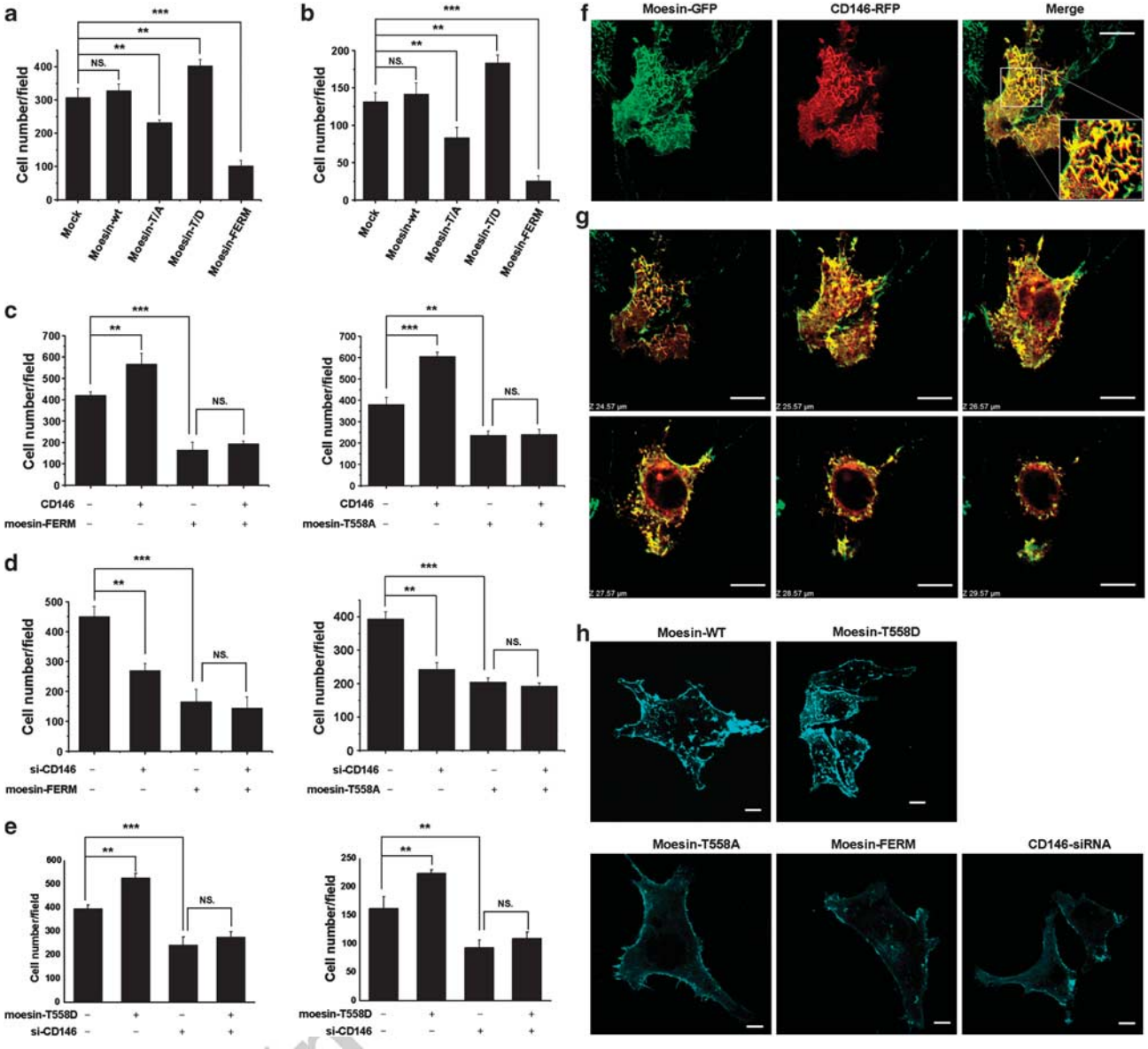

Figure 4 CD146/moesin association is required for CD146-induced melanoma cell migration. (**a**, **b**) Effects of various moesin mutants on melanoma cell motility were tested by migration assay using melanoma cells A375 (**a**) and SK-mel-28 (**b**). Each bar represents an individual transient transfectant of different moesin constructs (**$P<0.01$, ***$P<0.001$). (**c**–**e**) A375 cells were co-transfected with control siRNA or control plasmid, moesin-FERM, moesin-T558A or moesin-T558D, and WT CD146 or small interfering RNA duplexes targeting. Cells were then subjected to migration assays. The relative index is shown as the mean ± s.d. ($n=3$). (**f**) Colocalization of CD146 with moesin on microvilli of A375 cells. CD146-RFP and moesin-GFP were co-transfected into A375 cells. At 24 h after transfection, live cells were applied to laser scanning confocal microscopy (LSCM) analysis. The color of yellow indicates the overlapping of CD146-RFP and moesin-GFP signals. Scale bar, 10 μm. (**g**) A sequence of six optical sections at 1 μm interval obtained by the confocal analysis of A375 cells in (**e**). The most bottom sections (upper left) to the most up sections (lower right) are shown. (**h**) A375 cells were transfected with GFP-tagged moesin constructs or co-transfected with small interfering RNA duplexes targeting and moesin-GFP. At 24 h after transfection, live cells were applied to LSCM analysis for the localization of CFP signal on cell microvilli.

the merged channel (Figure 4f). Sequential optical sections of a defined region displayed a wide and significant overlapping of the CD146 with moesin fluorescent signals specifically in the membrane protrusions (Figure 4g). However, neither moesin-FERM nor moesin-T558A could be observed in these membranous protrusions and overexpression of them severely impaired microvilli formation, featured as much less and shorter branchlets or filopodia-like protrusions (Figure 4h). These data indicated that the intact structure and open conformation of moesin is required for appropriate local cytoskeleton rearrangement. Importantly, silencing CD146 expression by small interfering RNA (siRNA) significantly disturbed the normal distribution of WT moesin and disrupted the organization of microvilli-like structures (Figure 4h), suggesting that CD146 may serve critical functions in recruiting moesin, remodeling local actin filaments and

facilitating the formation of membrane protrusions during cell movements.

CD146 induces ERM phosphorylation through RhoA activity

Rho family of small GTPases are believed to regulate ERM protein functions by facilitating the phosphorylation of ERM CT domain, which leads to the disruption of self-association and release of membrane-binding NT domain (Bretscher *et al*., 2002; McClatchey, 2003). Here, we found that ectopic expression of a dominant-negative mutant of RhoA, RhoA-19N, remarkably suppressed the phosphorylation of ERM proteins and abolished the association between moesin and CD146 in SK-mel-28 cells (Figures 5a and b). Moreover, C3 transferase, which specifically ribosylates RhoA and renders it inactive, also significantly blocked ERM phosphorylation (Figure 5c). These results indicated that RhoA GTPase activity is crucial for activating moesin and inducing CD146/ERM interaction.

Unexpectedly, overexpression of CD146 was able to increase the phosphorylation level of ERM proteins apparently, but this enhancement was completely blocked by the treatment of C3 transferase (Figure 5c) or the overexpression of RhoA-19N (Figure 5d) in SK-mel-28 cells. In A375 cells, which have a relatively high

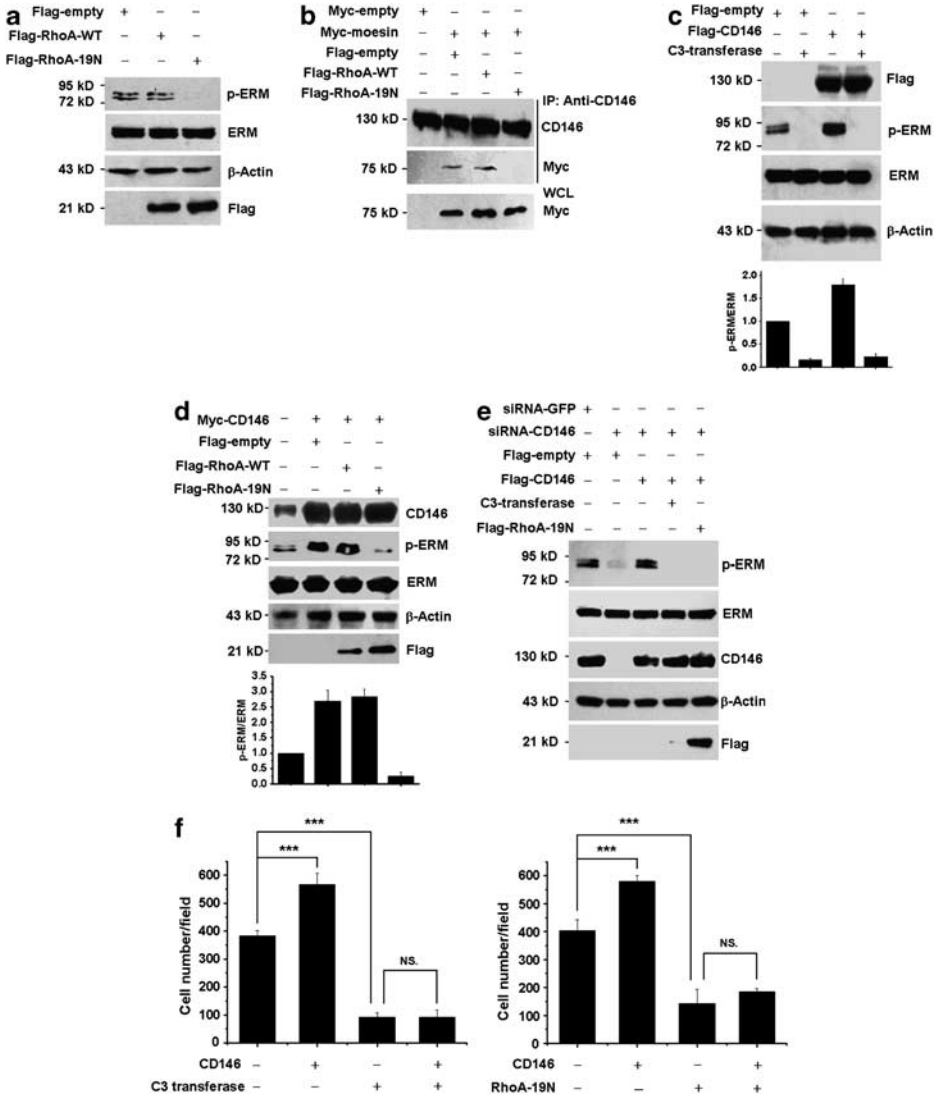

Figure 5 RhoA is required for CD146 induced ERM activation and cell migration. (**a**, **b**) RhoA is required for endogenous ERM phosphorylation and CD146/ERM association. (**a**) The control vector, RhoA-WT and RhoA-19N were transfected into SK-mel-28 cells. Immunoblot was performed using specific anti-p-ERM antibody. (**b**) The interaction of CD146 with Myc-moesin was determined by immunoprecipitation with mAb AA1 and immunoblot with anti-Myc mAb 9E10. (**c**, **d**) Rho GTPase is required for CD146-induced moesin activation *in vivo*. SK-mel-28 cells were treated with C3 transferase (**c**) or transfected with plasmid expressing dominant-negative RhoA-19N (**d**). Immunoblot for p-ERM levels and the quantification of relative p-ERM/ERM index are shown. At least three independent assays were performed. (**e**) CD146-expressing vector, Flag-CD146, was co-transfected with siRNA-CD146 to restore the expression of CD146 in A375 cells. Cells were then treated with C3 transferase or transfected with RhoA-19N. Immunoblot was performed using specific anti-p-ERM antibody. (**f**) A375 cells, treated with C3 transferase or co-transfected with plasmids expressing CD146 and RhoA-19N, were subjected to Transwell assays. The relative index is shown as the mean ± s.d. ($n = 3$) (***$P < 0.001$).

CD146 level, knockdown of CD146 by RNA interference almost completely diminished ERM phosphorylation, whereas the subsequent restoration of CD146 expression rescued the p-ERM level in a RhoA-dependent manner (Figure 5e). Moreover, a correlation between the amount of CD146 protein and the p-ERM level was observed in five independent melanoma cell lines (Figure 1b). Functionally, the ability of CD146 to promote melanoma cell migration also requires RhoA activity, as CD146 overexpression was unable to increase cell motility if endogenous RhoA was inhibited by C3 transferase or RhoA-19N (Figure 5f). Similar results were obtained in both A375 and SK-mel-28 cells. Therefore, these data interestingly indicated that CD146 could enhance the phosphorylation of ERM through RhoA GTPase, and RhoA has an important role in mediating CD146-induced melanoma cell migration by activating ERM proteins. Importantly, these results are consistent with previous findings that Rho GTPases mediate cytoskeleton rearrangement and contribute to cancer cell migration (Masiero *et al*., 1999; Worthylake and Burridge, 2003; Gadea *et al*., 2007).

RhoA-PI4P5K-PIP$_2$ pathway mediates CD146-induced ERM activation

At the downstream of RhoA, Ser/Thr kinases Rho-associated coiled-coil protein kinase (ROCK) and phosphatidylinositol-4-phosphate-5-kinase (PI4P5K) have been shown to regulate ERM phosphorylation and its interactions (Shibasaki *et al*., 1997; Matsui *et al*., 1999; Saci and Carpenter, 2005). Moreover, Rho-PI4P5K-PIP$_2$ pathway is responsible for continuous activation of ERM proteins. PI4P5K synthesizes PIP$_2$ and accumulates it on the membrane, and binding of PIP$_2$ to ERM proteins is a prerequisite for their phosphorylation and activation (Mangeat *et al*., 1999; Tsukita and Yonemura, 1999).

Therefore, we next used chemical inhibitors to test which kinase is involved in regulating ERM activity and CD146/ERM association in melanoma cells. ERM activation level was assayed by measuring the ratio of ERM proteins presented in the insoluble membrane-associated fraction of cell lysates to that in the soluble fraction. We found both neomycin, an inhibitor of PIP$_2$, and C3 transferase were able to considerably suppress ERM activation, whereas the ROCK inhibitor, Y27632, had little effect (Figure 6a). Moreover, only neomycin but not Y27632 could markedly abolish the association between CD146 and ERM proteins (Figure 6b). These data indicated that PIP$_2$ is required for activating ERM and maintaining CD146/ERM interaction.

As PIP$_2$ is synthesized by PI4P5K, we used specific siRNA duplex against PI4P5K to show it is indeed involved in the activation of ERM. Knockdown of

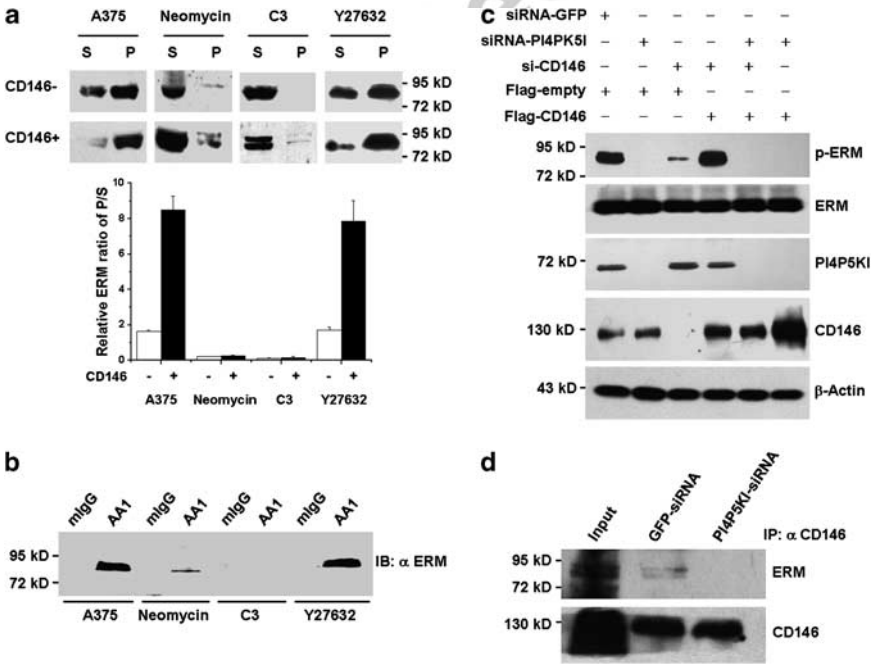

Figure 6 CD146 induces ERM activation through RhoA-PI4P5K-PIP$_2$ pathway. (**a**) A375 cells incubated with or without C3 transferase, Y27632 or neomycin, were homogenized in physiological solution and then divided into soluble supernatant (S) and insoluble pellet (P) fractions by centrifugation. ERM proteins were detected by immunoblot with mAb 38/87. The bar graph represented at least three independent tests and presented as the relative ratio of ERM proteins in pellet versus supernatant. (**b**) A375 cells untreated or treated with C3 transferase, Y27632 or neomycin, were immunoprecipitated by anti-CD146 mAb AA1, and each immunoprecipitate was immunoblotted with anti-ERM mAb 38/87. (**c**) CD146-expressing vector, Flag-CD146, was co-transfected with siRNA-CD146 to restore the expression of CD146 in A375 cells. Cells were then transfected with siRNA targeting PI4P5KI or control siRNA, and Flag-CD146 or control vector. At 48 h after transfection, cells lysates were immunoblotted with indicated antibodies. (**d**) A375 cells transfected with siRNA targeting PI4P5KI or control siRNA were immunoprecipitated by anti-CD146 mAb AA1, and each immunoprecipitate was immunoblotted with anti-ERM mAb 38/87. A measure of 30 μl of A375 cell lysate was set as the input lane.

PI4P5K abolished ERM phosphorylation and eliminated the interaction of CD146 with ERM proteins in A375 cells (Figures 6c and d). Same results were also obtained in SK-mel-28 cells (Supplementary Figure S7). These data suggested that PI4P5K is the essential effector kinase downstream of RhoA GTPase, and RhoA-PI4P5K-PIP_2 cascade is responsible for activating ERM proteins and inducing CD146/ERM association. Importantly, the same pathway is also required for CD146-induced ERM activation, as overexpression of CD146 could no longer enhance membrane translocation or phosphorylation of ERM in the presence of RhoA inhibitors or PIP_2 inhibitors or PI4P5K-specific siRNA (Figures 6a and c).

CD146/ERM association is required for CD146-induced RhoA activation and melanoma cell migration

The involvement of RhoA in CD146-induced ERM phosphorylation led us to investigate whether CD146 could directly induce the RhoA activation, which in turn regulates ERM proteins, in melanoma cells. Biochemical Rhotekin-Rho-binding domain (RBD) pull-down assay was used to analyze the activation state of RhoA by specifically measuring the level of GTP-bound RhoA proteins. The method was first verified by the observation that C3 transferase completely abrogated the activation of RhoA (Supplementary Figure S8). We found a close correlation between CD146 expression levels and the levels of active RhoA-GTP and p-ERM in SK-mel-28 cells, which indicated that CD146 indeed promotes ERM phosphorylation through inducing RhoA activation (Figure 7a).

More interestingly, the ability of CD146 to activate RhoA requires its physical interaction with ERM proteins. Western blot results showed that CD146-ΔKKGK, which lacks the ERM-binding motif, was unable to upregulate either RhoA activation or ERM phosphorylation level, whereas CD146-KKGKLP could significantly increase the levels of RhoA-GTP and p-ERM (Figures 7b and c). Moreover, dominant-negative moesin T588A and FERM blocked CD146-induced RhoA activation, meaning that the recruitment of functional ERM to CD146 is essential for activating RhoA (Figure 7d). These data suggested that CD146 could activate the RhoA GTPase by interacting with ERM proteins and therefore induce further ERM phosphorylation and activation.

Given the finding that the moesin-binding KKGK motif is not only needed for recruiting moesin, but also critical for activating RhoA, we next examined the importance of this motif in promoting cell migration. By testing the transmigration capabilities of the melanoma cells transfected with CD146-wt, CD146-KKGKLP or CD146-ΔKKGK, we found that loss of KKGK motif significantly diminished the function of CD146 in enhancing cell migration in both A375 and SK-mel-28 cells (Figures 7e and f). More importantly, CD146 mutant having only the KKGK motif in the cytoplamic tail is sufficient to induce RhoA activation and promote cell migration, suggesting that the function of CD146 in initiating cellular signaling may entirely rely on its interaction with ERM proteins.

These results together indicated that the interaction between CD146 and ERM proteins not only links CD146 to actin filaments, but also initiates a signaling cascade, which activates RhoA-PI4P5K-PIP_2 pathway, leading to the activation of more ERM proteins, strengthening of CD146 anchorage to cytoskeletons and eventually cell movements.

CD146/ERM complex associates with RhoGDI1 and promotes RhoA activation

Although it was found that CD146 could induce RhoA activation through recruiting moesin, the mechanism of how CD146/ERM complex activates RhoA was still unexplored. The activation of Rho is known to be mediated by three distinct functional classes of regulatory proteins, namely Rho guanine nucleotide exchange factors, Rho GTPase-activating proteins and RhoGDIs (Oleksy *et al*., 2006; Ridley, 2006; Boureux *et al*., 2007). By re-examining the CD146/ERM complex in A375 and SK-mel-28 cells, we found that CD146 was also co-imunoprecipitated with RhoGDI1 (Figure 8a). Subsequent confocal microscope analysis showed very clear fluorescent colocalization of CD146 with RhoGDI1 on the membrane of A375 cells (Figure 8b). Moreover, the CD146/RhoGDI1 interaction was also confirmed in other two melanoma cell lines, Mel-624 and Mel-888^{CD146} (data not shown), indicating that the association might be common and conserved in human melanoma cells.

We then tested whether the binding of RhoGDI1 to CD146 requires functional ERM proteins. It was found that the interaction between RhoGDI1 and CD146 was markedly diminished in cells expressing dominant-negative moesin T558A and severely impaired in the presence of moesin-FREM (Figure 8c). Moreover, interactions between RhoGDI1 and moesin T588D were also directly detected by co-immunoprecipitation, whereas RhoGDI1 did not bind to inactive moesin T588A, implying that an active conformation of moesin is needed for RhoGDI1/ERM interaction (Figure 8d). However, RhoGDI1 also bound to the FERM domain of moesin alone, although the binding was not as strong as its association with moesin T588D (Figure 8d). The results interestingly indicated that although the NT domain of moesin has RhoGDI1 binding site, it might be insufficient to mediate CD146/RhoGDI1 interaction, whereas the C terminus in active form would contribute to stabilizing the CD146/moesin/RhoGDI1 complex. Taken together, these data suggested that moesin mediates an indirect association of RhoGDI1 with CD146 cytoplasmic tail.

As shown in Figure 8b, overexpression of CD146 in A375 cells apparently induced subcellular translocation of RhoGDI1 from the cytoplasm to the membrane (comparing the cell expressing both RhoGDI1-GFP and CD146-RFP with the one expressing only RhoGDI1-GFP). We further confirmed this biochemically by showing the increase of RhoGDI1 in the insoluble

fraction of cell lysate upon CD146 overexpression, and found that active moesin is required for the translocation of RhoGDI1 to the membrane (Figure 8e). These results supported the recruitment of RhoGDI1 by CD146/moesin complex. The subsequent question was how the formation of CD146/moesin/RhoGDI1 ternary complex affected the activity of RhoA. In A375 cells transfected with empty vectors, RhoGDI1 was found

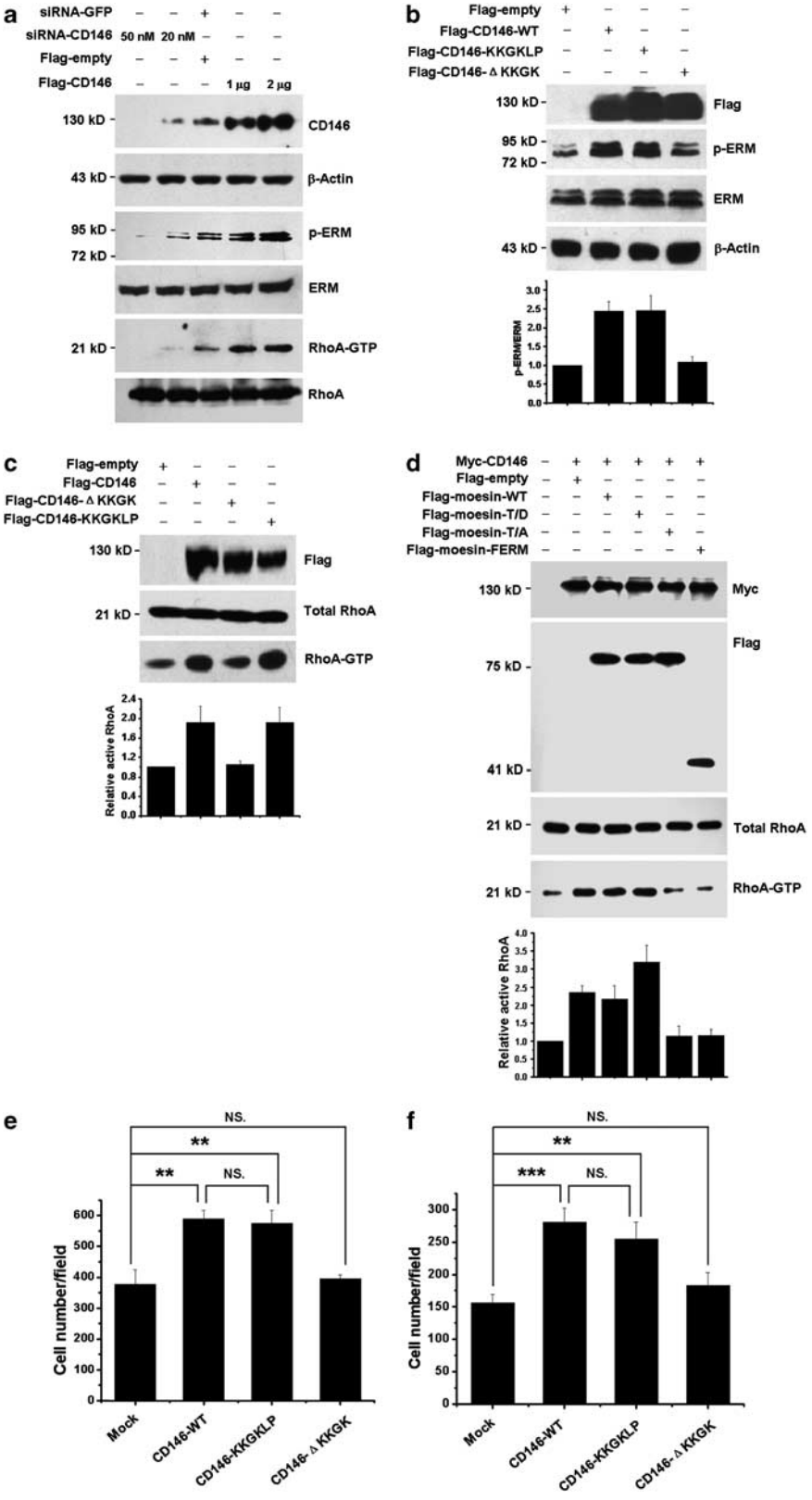

retained in a complex with RhoA; however, RhoGDI1 was no longer associated with RhoA upon ectopic expression of CD146 (Figure 8f). Importantly, CD146 mutant without the moesin-binding KKGK motif was unable to sequester RhoGDI1 from RhoA, bolstering further that the binding of moesin to CD146 is crucial for sheltering RhoGDI1 in a membrane-linked complex and preventing the inhibitory association of RhoGDI1 with RhoA.

We then co-expressed RhoGDI1 with CD146 in A375 cells and examined the transmigration capacities of cancer cells. Under the overexpression of RhoGDI1, CD146 was not able to promote cell migration any longer (Figure 8g). We reasoned that the ability of CD146 to recruit RhoGDI1 to the membrane was limited. Thus, ectopically expressed RhoGDI1 proteins could not be completely pulled out from the cytosolic pool, and the remaining RhoGDI1 was able to inhibit endogenous RhoA activity, resulting in compromised cell motility. The prevention of CD146-induced cell movements by increased level of RhoGDI1 indicated that regulating the subcellular localization of RhoGDI1 is an essential step of CD146 signaling cascade during cytoskeleton remodeling. To sum up, the functional consequences of forming CD146/moesin/RhoGDI1 heterotrimer are the release of RhoA activity from RhoGDI1-mediated inhibition, and the subsequent enhancement of cell migration mediated by activated RhoA.

Discussion

CD146 overexpression has been shown correlated with metastatic potential of human melanoma and capable of promoting cancer cell migration and invasion in both clinical studies and laboratory experiments (Bani *et al*., 1996; Shih *et al*., 1997; Xie *et al*., 1997). However, the exact mechanism of how CD146 is involved in cell movements still remains largely unknown. Here, in human melanoma cells we uncovered the association between CD146 and ERM proteins, which leads to cytoskeleton remodeling and eventually cell migration mainly by two ways. First, ERM proteins, serving as adaptors, link membrane CD146 to actin filaments, which gives rise to local cytoskeleton rearrangement and promotes the formation of specific cell protrusions, such as microvilli and filopodia. Second, the interaction of CD146 with ERM proteins induces the activation of RhoA by recruiting RhoGDI to the CD146/ERM complex and sequestering it from RhoA spatially. Release of RhoA from the inhibitory interaction with RhoGDI results in upregulated RhoA activity, which then triggers various downstream signaling, contributing to global microfilament reorganizations. One of these signal events is the activation of PI4P5K-PIP_2 pathway, which induces further phosphorylation and activation of ERM proteins, forming a positive feedback loop to reinforce the association between CD146 and ERM proteins. The model we proposed here provides a novel mechanism of CD146 promoting melanoma cell migration.

On the basis of our observations that CD146 induces the formation and elongation of microvilli by recruiting ERM proteins and actin filaments, we propose that cell protrusion-enriched CD146 in collaboration with activated ERM proteins mediates the local cytoskeleton remodeling and microvillar development in specific membrane regions at the leading edge of the cell during cell migration. This notion is supported by recent discoveries that upon a gradient of CXCL12 concentrations CD146 could be polarly redistributed to mediate Wnt5a-controlled melanoma cell polarity and directional movement (Witze *et al*., 2008). A similar CD146–actin–myosin polarity structure was also found asymmetrically accumulated in the cell periphery under the treatment of CXCL12 gradient. Our studies close the gap between CD146 and actin filament and further bolster the idea that in response to chemokines CD146 can be first polarized in the direction of membrane extension, and then serves as an organizer to recruit cytoskeleton and motor proteins to specialized domains of the differentiated membrane. These molecular events cause local cytoskeleton rearrangement, cell protrusion formation, microvilli elongation, polarized membrane growth and eventually directional cell movement.

It is of great interest that CD146 not only recruits ERM proteins, but also induces ERM phosphorylation and activation. Previous studies have identified two steps for stable activation of ERM proteins (Niggli and Rossy, 2008). ERM proteins first interact via their N-terminal FERM domain with the membrane PIP_2. Subsequently, kinases, such as protein kinase C and ROCK, catalyze the C-terminal phosphorylation on a conserved threonine residue, which results in disruption of the intramolecular associations and exposure of NT domain. Our study found that RhoA-PI4P5K pathway, which upregulates the PIP_2 level, is essential for both endogenous CD146/ERM association and CD146 overexpression-induced ERM activation. However,

Figure 7 CD146/ERM association is required for CD146-induced RhoA activation and melanoma cell migration. (**a**) SK-mel-28 cells were transfected with CD146-siRNA or plasmids expressing CD146. At 48 h after transfection, immunoblot was performed using specific anti-p-ERM antibody. The active RhoA-GFP level was detected by GST-RBD pull-down assays. (**b**, **c**) SK-mel-28 cells were transfected with constructs expressing various Flag-tagged CD146 mutants. Immunoblot of p-ERM levels (upper) and the quantification (lower) of relative p-ERM/ERM index are shown as the mean ± s.d. ($n=3$) (**b**). Cells were subjected to Rhotekin-RBD pull-down assays. The relative ratio of active RhoA to total RhoA is shown as the mean ± s.d. ($n=3$) (**c**). (**d**) Cells were transfected with constructs expressing CD146 or various Flag-tagged moesin mutants. At 48 h after transfection, cells were subjected to Rhotekin-RBD pull-down assays. The relative ratio of active RhoA to total RhoA is shown as the mean ± s.d. ($n=3$). (**e**, **f**) A375 (**e**) or SK-mel-28 cells (**f**) were transfected with constructs expressing various Flag-tagged CD146 mutants. At 48 h after transfection, cells were subjected to Transwell assays. The relative index is shown as the mean ± s.d. ($n=3$) (**$P<0.01$, ***$P<0.001$).

Rho-activated ROCK is not responsible for ERM phosphorylation in human melanoma cells, indicating the function of ROCK as a kinase for the Thr residue of ERM proteins might depend on cell types (Hebert *et al*., 2008). Moreover, various specific inhibitors against protein kinase Cs (BIM and Gö6976), PI3-kinase

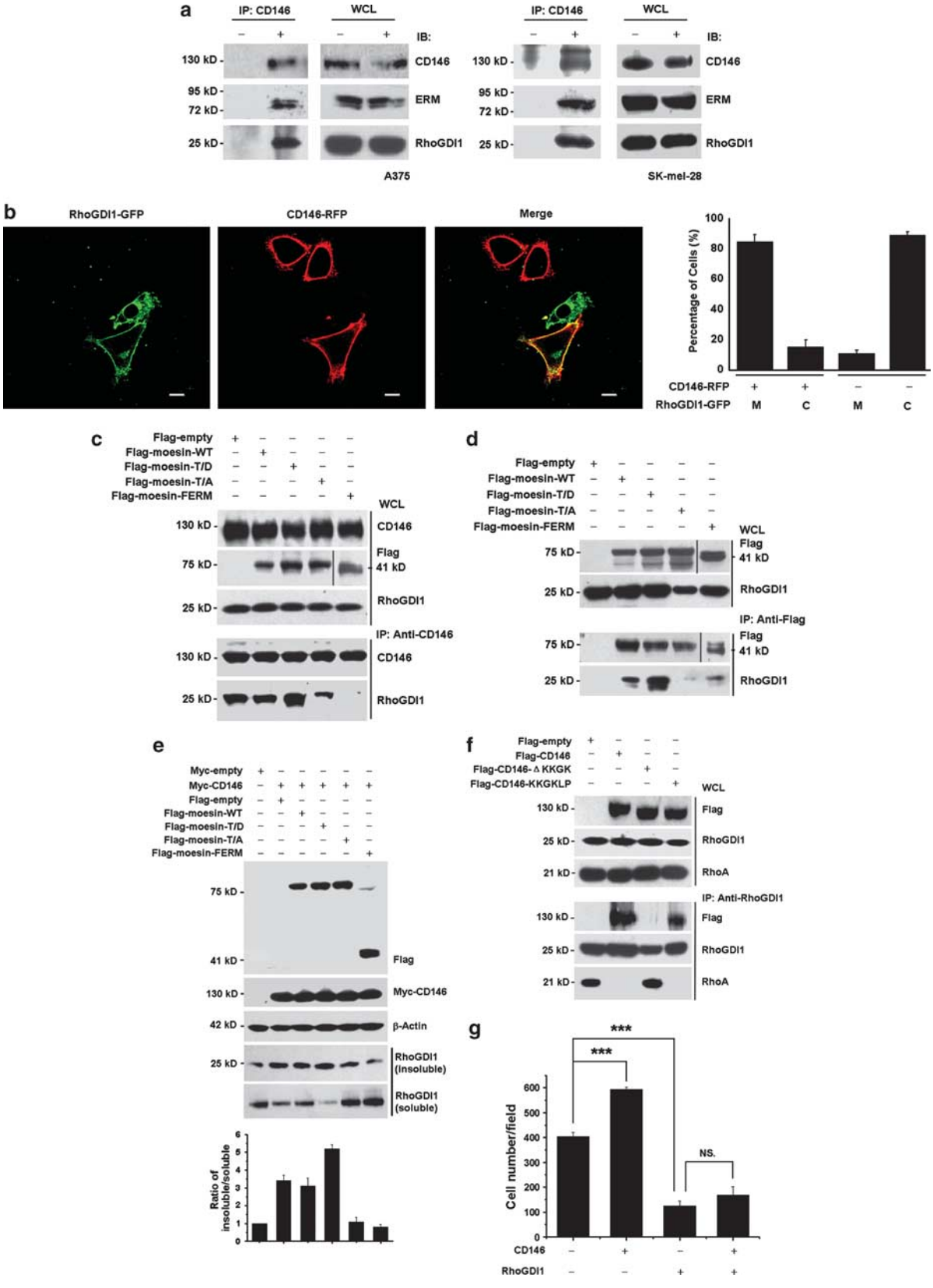

(LY294002) or p38 mitogen-activated protein kinase (SB203580) have no significant effect on ERM activation and cell morphology (data not shown), suggesting that some unidentified enzymes might be involved in catalyzing Thr phosphorylation of ERM CT domain in human melanoma cells. Nevertheless, CD146-induced increase of PIP_2 level raises more phosphorylated and activated ERM proteins, which strengthen the connection between CD146 and actin filament, reinforcing cytoskeleton rearrangement in an auto-regulatory manner.

Another surprising discovery in this study is that except for serving as a docking site for F-actin, CD146-bound ERMs also initiate a signaling cascade to activate RhoA by releasing it from the inhibitory interaction with RhoGDI. In melanoma cells, in response to ectopic expression of CD146, RhoGDI is recruited and then sequestered in a CD146/moesin/RhoGDI ternary complex by its interaction with the NT domain of ERM proteins, which leads to the dissociation of RhoA from GDI and subsequent conversion of inactive RhoA-GDP to active RhoA-GTP by guanine nucleotide exchange factors on the membrane. Actually the exactly same mechanism was also found previously in ERM-CD44 system *in vitro* (Takahashi *et al*., 1997), indicating that membrane receptor-bound ERM proteins may have a general activity to sequester GDI and activate Rho GTPase. As the function of RhoA in regulating cytoskeleton reorganization and promoting cell migration had been validated before in melanoma cells (Yang *et al*., 2006; Bartolome *et al*., 2008; Molina-Ortiz *et al*., 2009), CD146-inducing RhoA activation could upregulate the global capability of remodeling cell scaffolding and promoting cell movements. On the basis of these findings, our studies provide a mechanistic view for the correlation between CD146 overexpression and increased cell motility in human melanoma and may offer therapeutic targets for preventing cancer metastasis.

Materials and methods

Antibodies and reagents

The following antibodies were used in this study: anti-CD146 rabbit polyclonal antibody, mAb AA1 and AA14 (generated in our laboratory), anti-FLAG (clone M2), anti-His-tag, and anti-β-actin (Sigma-Aldrich, St Louis, MO, USA), anti-PI4P5K, anti-Myc (9E10) and anti-RhoGDI1 (Santa Cruz Biotechnology, Santa Cruz, CA, USA), anti-GFP and anti-ERM 38/87 (Abcam, Cambridge, MA, USA), anti-phospho-ERM, and anti-RhoA (Cell Signaling, Danvers, MA, USA), horseradish peroxidase-conjugated anti-mouse and anti-rabbit secondary antibodies (GE Healthcare, Piscataway, NJ, USA). All western blots were carried out using enhanced SuperSignal West Dura (Pierce, Rockford, IL, USA). The inhibitors used were 10 μM Y27632 (Sigma-Aldrich), 1 mM neomycin (Sigma-Aldrich) and 1 μg/ml cell-permeable Rho inhibitor the exoenzyme C3-transferase (Cytoskeleton, Denver, CO, USA).

Plasmids and siRNA duplex

Flag-CD146 and Myc-CD146 has been described previously (Zheng *et al*., 2009). The Flag-CD146-KKGKLP, Flag-CD146-ΔKKGK and GST-CD146cyt mutants were generated by a polymerase chain reaction-based approach using Flag-CD146 as a template. WT Flag-ezrin, Flag-radixin, Flag-moesin, GFP-moesin, CFP-moesin, Myc-moesin, His-moesin-FERM (residues 1–320), Flag-moesin-FERM and GST-RBD were generated by a polymerase chain reaction-based approach using A375 cell cDNA as a template. Flag-moesin-T558A and Flag-moesin-T558D were generated by site-directed mutagenesis using WT Flag-moesin as a template. CFP-moesin-T558A, CFP-moesin-T558D and CFP-moesin-FERM mutants were generated by replacing WT CFP-moesin with the corresponding fragments of Flag-moesin-T558A, Flag-moesin-T558D and Flag-moesin-FERM. Flag-RhoA, Myc-RhoGDI1 and GFP-RhoGDI1 were generated by a polymerase chain reaction-based approach using A375 cell cDNA as a template. Flag-RhoA-19N was generated by site-directed mutagenesis using WT Flag-RhoA as a template. The fidelity and appropriate mutations of all the constructs generated were confirmed by sequencing.

The synthetic siRNA duplex targeting PI4P5K1 were generated according to the sequences reported previously (Lacalle *et al*., 2007; Barrero-Villar *et al*., 2008). The synthetic small interfering RNA duplexes targeting CD146 and GFP control, respectively, were synthesized at Invitrogen (San Diego, CA, USA) using the sequences reported previously (Zheng *et al*., 2009). The efficacy of gene silencing was analyzed by immunoblotting and found to be optimal at 24 h after siRNA transfection.

Cells and transfection

Human melanoma cell lines A375, SK-mel-28 and Mel-624 were obtained from American Type Culture Collection

Figure 8 CD146/ERM complex associates with RhoGDI1 and promotes RhoA activation. (**a**) Co-immunoprecipitation (Co-IP) assays for association of endogenous RhoGDI1 and ERM proteins with CD146 in A375 and SK-mel-28 cells. Cell lysates were immunoprecipitated by AA1 and probed with 38/87 and anti-RhoGDI1 antibody. Approximately 1% of the whole-cell lysate was loaded as positive control. (**b**) Colocalization of CD146 with RhoGDI1 on cell membrane. A375 cells were transfected with CD146-RFP and RhoGDI1-GFP, and were applied to laser scanning confocal microscopy (LSCM) analysis. Scale bar, 10 μm. The relative ratio of cells with membrane localization and cytoplasmic localization is shown as the mean ± s.d. ($n=3$) at the right panel. In all, 13 different fields with total cell number of approximately 4937 were counted. (**c**) A375 cells were transfected with constructs expressing various Flag-tagged moesin mutants. Cell lysates were immunoprecipitated by AA1 and probed with anti-RhoGDI1 antibody. (**d**) A375 cells were transfected with constructs expressing various Flag-tagged moesin mutants. Cell lysates were immunoprecipitated by anti-Flag M2 and probed with anti-RhoGDI1 antibody. (**e**) A375 cells were transfected with constructs expressing various Flag-tagged moesin mutants. The soluble and insoluble RhoGDI1 proteins were recovered by centrifugation in physiological solution. The amount of RhoGDI1 proteins in pellet and supernatant was quantified by immunoblot using RhoGDI1. The relative ratio of RhoGDI1 in insoluble/soluble is shown as the mean ± s.d. ($n=3$). (**f**) A375 cells were transiently transfected with constructs expressing various Flag-tagged CD146 mutants. Cell lysates were immunoprecipitated by anti-RhoGDI1 antibody, and immunoprecipitates were probed with anti-RhoGDI1, anti-RhoA and anti-Flag antibodies. Approximately 1% of the whole-cell lysate was loaded as positive control. (**g**) A375 cells were transfected with RhoGDI1 or CD146 alone or co-transfected with RhoGDI1 and CD146. At 48 h after transfection, cells were subjected to Transwell assays. The relative index is shown as the mean ± s.d. ($n=3$) (***$P<0.001$).

(Rockville, MD, USA). A375, Mel-624 and SK-mel-28 are natively CD146-expressing cells, whereas Mel-888^{CD146} was a stably transfected CD146-expressing cell line. All cell lines were cultured in Dulbecco's modified Eagle medium supplemented with 10% fetal calf serum and antibiotics (Gibco Life Technologies Inc., Paisley, UK). All cultures were performed in 5% CO_2 humidified atmosphere at 37 °C. Cells were cultured on glass coverslips pretreated with 50 μg/ml poly-L-lysine for fluorescence microscopy studies. The Lipofectamine 2000 reagent- (Invitrogen) mediated transfection was performed according to the manufacturer's instructions.

Immunoprecipitation
Cells were lysed with radioimmunoprecipitation assay buffer (150 mM NaCl, 50 mM Tris, pH 8.0, 0.1% sodium dodecyl sulfate (SDS), 0.5% deoxycholate, 1% NP-40, 1 mM phenylmethanesulfonyl fluoride and Protease Inhibitor Cocktails (Roche, Indianapolis, IN, USA)) for 0.5 h on ice. After centrifugation, the soluble supernatants were pre-cleared with protein G PLUS-Agarose (Santa Cruz Biotechnology Inc.). Samples were then immunoprecipitated with specific antibodies and 25 μl of protein G-agarose beads. Protein G-bound immunocomplexes were extensively washed with radioimmunoprecipitation assay washing buffer (150 mM NaCl, 50 mM Tris, pH 8.0, 0.1% SDS, 0.5% deoxycholate, 0.1% NP-40, 1 mM phenylmethanesulfonyl fluoride and Protease Inhibitor Cocktails) and boiled in sample loading buffer for SDS–polyacrylamide gel electrophoresis. The immunoprecipitated proteins were detected by western blot.

To identify potential CD146-associated proteins, 1 ml of lysate from 6×10^6 A375 cells was prepared and immunoprecipitated with anti-CD146 mAb AA98. Proteins bound to protein G-agarose beads were separated by 10% SDS–polyacrylamide gel electrophoresis and stained with Coomassie blue, and proteins specifically associated with CD146 was analyzed using mass spectrometry.

Immunoblot analysis
For immunoblot, proteins were resolved with 10% SDS–polyacrylamide gel electrophoresis and then transferred to a nitrocellulose membrane (Amersham, Piscataway, NJ, USA). The membranes were blocked with 5% non-fat milk in phosphate-buffered saline with 0.1% Tween-20 for 2 h, incubated for 2 h with primary antibodies and then probed with horseradish peroxidase-conjugated anti-mouse or anti-rabbit secondary antibodies. All immunoblots were carried out using chemiluminescence reagent (Pierce) and exposed to X-ray films (Kodak, New York, NY, USA).

In vitro *GST pull-down assay*
In all, 0.15 μg GST or GST-CD146cyt expressed in *Escherichia coli* was absorbed on glutathione agarose beads (Sigma-Aldrich). The beads were then incubated with 0.15 μg purified moesin-FERM-His protein for 1 h in the presence or absence of anti-CD146 mAbs. Proteins bound to the beads were then boiled in sample loading buffer and subjected to immunoblot.

Treating living cells with inhibitors
A375 cells cultured to 70–80% confluence were incubated with or without 1 μg/ml C3 transferase, 10 μM Y27632 and 1 mM neomycin, for 6, 12 and 48 h, respectively. To compare the amounts of soluble and insoluble ERM proteins, cells were homogenized in a physiological solution (130 mM KCl, 20 mM NaCl, 1 mM $MgCl_2$, 10 mM Hepes, pH 7.5, 1 mM phenylmethanesulfonyl fluoride and Protease Inhibitor Cocktails). After centrifugation at 300 000 *g* for 20 min, the amount of ERM proteins in pellet and supernatant was quantified by immunoblot using anti-ERM 38/87. At least three independent experiments were performed. In addition, cells under the same treatments were also lysed and then immunoprecipitated with anti-CD146 mAb AA1, and the precipitates were separated by SDS–polyacrylamide gel electrophoresis followed by immunoblot with anti-ERM 38/87.

Pull-down assay for the determination of RhoA activation
Cells were lysed in 600 μl radioimmunoprecipitation assay buffer, and an aliquot of lysate (90 μl) was saved to test the total protein expression after centrifugation. The rest of lysates were incubated with GST-RBD (20 μg) beads at 4 °C for 45 min. Beads were washed four times with wash buffer (50 mM Tris, pH 7.6, 1% Triton X-100, 500 mM NaCl, 50 mM $MgCl_2$, 0.1 mM phenylmethanesulfonyl fluoride and Protease Inhibitor Cocktails). Bound Rho proteins were detected by immunoblot using an mAb against RhoA (Cell Signaling Technology). The amount of RBD-bound RhoA was normalized to the total amount of RhoA in cell lysates for the comparison of RhoA activity (level of GTP-bound RhoA) in different samples. At least three independent experiments were performed.

Immunofluorescence
For immunofluorescent staining, A375 cells were plated on coverslips. After transfections, the cells were washed with phosphate-buffered saline, fixed in 4% paraformaldehyde/phosphate-buffered saline, permeabilized with 0.2% Triton X-100/phosphate-buffered saline and incubated with the indicated primary antibody, followed by incubation with FITC-conjugated anti-mouse immunoglobulin G or anti-rabbit immunoglobulin GG (Invitrogen). F-actin was stained by Alexa Fluor 488 phalloidin (Invitrogen) for 20 min at room temperature. Samples were examined with a confocal laser scanning microscope (Olympus, Tokyo, Japan).

Cell migration assay
Cell migration capabilities were assayed using Transwell (8-μm pore filters; Corning Costar, Lowell, MA, USA). Before migration, cells were serum-starved overnight. Then, 2.0×10^5 cells in 50 μl serum-free Dulbecco's modified Eagle's medium were added into the upper chamber, and 200 μl Dulbecco's modified Eagle's medium supplemented with 10% fetal calf serum was added to the lower chamber. Cells were allowed to migrate for 48 h at 37 °C. After removing cells on the upper surface of the filter using cotton swabs, cells that invaded through the membrane were fixed with 4% paraformaldehyde and stained with 0.1% crystal violet solution. The number of cells that reached the lower part of the Transwell filter membrane was counted and plotted as the number of cells per optic field (× 4). Experiments were carried out in triplicate.

Statistical analysis
All values are representative of experiments performed in triplicate. The graphical results are expressed as the mean ± s.d. Paired *t*-test methods were used to compare differences between groups in various experiments. The criterion for statistical significance is defined as $P < 0.05$.

Abbreviations

ERM proteins, ezrin–radixin–moesin proteins; PIP_2, phosphatidylinositol 4,5-biphosphate; RBD, Rho-binding domain;

RhoGDI1, Rho guanine nucleotide dissociation inhibitory factors 1; ROCK, Rho-associated coiled-coil protein kinase.

Conflict of interest

The authors declare no conflict of interest.

Acknowledgements

We thank Dr J Johnson for providing the CD146-transfected Mel-888^{CD146} cells and *CD146* gene contained in pUC-CD146 plasmids. This work is partly supported by grants from the National 863 Grant (2006AA02A245), the National Basic Research Program of China (973 Program) (2009CB521704, 2011CB933503), the National Important Science and Technology Specific Projects (2008ZX10004-005, 2008ZX10002-017, 2009ZX09102-247), the National Natural Science Foundation of China (91029732) and the Knowledge Innovation Program of the Chinese Academy of Sciences (KSCX2-YW-R-121, KSCX2-YW-R-173, KSCX2-YW-M15).

Author contributions: YL and CZ designed, carried out experi ments, analyzed data and wrote the paper. JZ performed experiments and carried out image analyses. DL, JZ and SX contributed to experimental design, data analysis and expertise. JF and DY contributed to experimental design and data analysis. XY designed the project, designed experiments and analyzed data.

References

Aldovini D, Demichelis F, Doglioni C, Di Vizio D, Galligioni E, Brugnara S *et al*. (2006). M-CAM expression as marker of poor prognosis in epithelial ovarian cancer. *Int J Cancer* **119**: 1920–1926.

Anfosso F, Bardin N, Frances V, Vivier E, Camoin-Jau L, Sampol J *et al*. (1998). Activation of human endothelial cells via S-endo-1 antigen (CD146) stimulates the tyrosine phosphorylation of focal adhesion kinase p125(FAK). *J Biol Chem* **273**: 26852–26856.

Bani MR, Rak J, Adachi D, Wiltshire R, Trent JM, Kerbel RS *et al*. (1996). Multiple features of advanced melanoma recapitulated in tumorigenic variants of early stage (radial growth phase) human melanoma cell lines: evidence for a dominant phenotype. *Cancer Res* **56**: 3075–3086.

Barreiro O, Vicente-Manzanares M, Urzainqui A, Yanez-Mo M, Sanchez-Madrid F. (2004). Interactive protrusive structures during leukocyte adhesion and transendothelial migration. *Front Biosci* **9**: 1849–1863.

Barrero-Villar M, Barroso-Gonzalez J, Cabrero JR, Gordon-Alonso M, Alvarez-Losada S, Munoz-Fernandez MA *et al*. (2008) PI4P5-kinase Ialpha is required for efficient HIV-1 entry and infection of T cells. *J Immunol* **181**: 6882–6888.

Bartolome RA, Wright N, Molina-Ortiz I, Sanchez-Luque FJ, Teixido J. (2008). Activated G(alpha)13 impairs cell invasiveness through p190RhoGAP-mediated inhibition of RhoA activity. *Cancer Res* **68**: 8221–8230.

Bidlingmaier S, He J, Wang Y, An F, Feng J, Barbone D *et al*. (2009). Identification of MCAM/CD146 as the target antigen of a human monoclonal antibody that recognizes both epithelioid and sarcomatoid types of mesothelioma. *Cancer Res* **69**: 1570–1577.

Boureux A, Vignal E, Faure S, Fort P. (2007). Evolution of the Rho family of ras-like GTPases in eukaryotes. *Mol Biol Evol* **24**: 203–216.

Bretscher A, Chambers D, Nguyen R, Reczek D. (2000). ERM-Merlin and EBP50 protein families in plasma membrane organization and function. *Annu Rev Cell Dev Biol* **16**: 113–143.

Bretscher A, Edwards K, Fehon RG. (2002). ERM proteins and merlin: integrators at the cell cortex. *Nat Rev* **3**: 586–599.

Bretscher A, Reczek D, Berryman M. (1997). Ezrin: a protein requiring conformational activation to link microfilaments to the plasma membrane in the assembly of cell surface structures. *J Cell Sci* **110**(Part 24): 3011–3018.

Bu P, Gao L, Zhuang J, Feng J, Yang D, Yan X. (2006). Anti-CD146 monoclonal antibody AA98 inhibits angiogenesis via suppression of nuclear factor-kappaB activation. *Mol Cancer Therap* **5**: 2872–2878.

Crepaldi T, Gautreau A, Comoglio PM, Louvard D, Arpin M. (1997). Ezrin is an effector of hepatocyte growth factor-mediated migration and morphogenesis in epithelial cells. *J Cell Biol* **138**: 423–434.

DerMardirossian C, Bokoch GM. (2005). GDIs: central regulatory molecules in Rho GTPase activation. *Trends Cell Biol* **15**: 356–363.

Dovas A, Couchman JR. (2005). RhoGDI: multiple functions in the regulation of Rho family GTPase activities. *Biochem J* **390**: 1–9.

Gadea G, de Toledo M, Anguille C, Roux P. (2007). Loss of p53 promotes RhoA-ROCK-dependent cell migration and invasion in 3D matrices. *J Cell Biol* **178**: 23–30.

Gervais L, Claret S, Januschke J, Roth S, Guichet A. (2008). PIP5K-dependent production of PIP2 sustains microtubule organization to establish polarized transport in the *Drosophila* oocyte. *Development (Cambridge, England)* **135**: 3829–3838.

Guezguez B, Vigneron P, Alais S, Jaffredo T, Gavard J, Mege RM *et al*. (2006). A dileucine motif targets MCAM-l cell adhesion molecule to the basolateral membrane in MDCK cells. *FEBS Lett* **580**: 3649–3656.

Hebert M, Potin S, Sebbagh M, Bertoglio J, Breard J, Hamelin J. (2008). Rho-ROCK-dependent ezrin–radixin–moesin phosphorylation regulates Fas-mediated apoptosis in Jurkat cells. *J Immunol* **181**: 5963–5973.

Hirao M, Sato N, Kondo T, Yonemura S, Monden M, Sasaki T *et al*. (1996). Regulation mechanism of ERM (ezrin/radixin/moesin) protein/plasma membrane association: possible involvement of phosphatidylinositol turnover and Rho-dependent signaling pathway. *J Cell Biol* **135**: 37–51.

Johnson JP, Bar-Eli M, Jansen B, Markhof E. (1997). Melanoma progression-associated glycoprotein MUC18/MCAM mediates homotypic cell adhesion through interaction with a heterophilic ligand. *Int J Cancer* **73**: 769–774.

Johnson JP, Rothbacher U, Sers C. (1993). The progression associated antigen MUC18: a unique member of the immunoglobulin supergene family. *Melanoma Res* **3**: 337–340.

Kristiansen G, Yu Y, Schluns K, Sers C, Dietel M, Petersen I. (2003). Expression of the cell adhesion molecule CD146/MCAM in non-small cell lung cancer. *Anal Cell Pathol* **25**: 77–81.

Lacalle RA, Peregil RM, Albar JP, Merino E, Martinez AC, Merida I *et al*. (2007) Type I phosphatidylinositol 4-phosphate 5-kinase controls neutrophil polarity and directional movement. *J Cell Biol* **179**: 1539–1553.

Lee JH, Katakai T, Hara T, Gonda H, Sugai M, Shimizu A. (2004). Roles of p-ERM and Rho-ROCK signaling in lymphocyte polarity and uropod formation. *J Cell Biol* **167**: 327–337.

Li G, Satyamoorthy K, Herlyn M. (2002). Dynamics of cell interactions and communications during melanoma development. *Crit Rev Oral Biol Med* **13**: 62–70.

Louvet-Vallee S. (2000). ERM proteins: from cellular architecture to cell signaling. *Biol Cell/Under Ausp Eur Cell Biol Org* **92**: 305–316.

Luca M, Hunt B, Bucana CD, Johnson JP, Fidler IJ, Bar-Eli M. (1993). Direct correlation between MUC18 expression and metastatic potential of human melanoma cells. *Melanoma Res* **3**: 35–41.

Luna EJ, Hitt AL. (1992). Cytoskeleton—plasma membrane interactions. *Science (New York, NY)* **258**: 955–964.

Mangeat P, Roy C, Martin M. (1999). ERM proteins in cell adhesion and membrane dynamics. *Trends Cell Biol* **9**: 187–192.

Masiero L, Lapidos KA, Ambudkar I, Kohn EC. (1999). Regulation of the RhoA pathway in human endothelial cell spreading on type IV collagen: role of calcium influx. *J Cell Sci* **112**(Part 19): 3205–3213.

Matsui T, Yonemura S, Tsukita S, Tsukita S. (1999). Activation of ERM proteins *in vivo* by Rho involves phosphatidylinositol 4-phosphate 5-kinase and not ROCK kinases. *Curr Biol* **9**: 1259–1262.

McClatchey AI. (2003). Merlin and ERM proteins: unappreciated roles in cancer development? *Nat Rev Cancer* **3**: 877–883.

McClatchey AI, Fehon RG. (2009). Merlin and the ERM proteins—regulators of receptor distribution and signaling at the cell cortex. *Trends Cell Biol* **19**: 198–206.

Molina-Ortiz I, Bartolome RA, Hernandez-Varas P, Colo GP, Teixido J. (2009). Overexpression of E-cadherin on melanoma cells inhibits chemokine-promoted invasion involving p190RhoGAP/p120ctn-dependent inactivation of RhoA. *J Biol Chem* **284**: 15147–15157.

Niggli V, Rossy J. (2008). Ezrin/radixin/moesin: versatile controllers of signaling molecules and of the cortical cytoskeleton. *Int J Biochem Cell Biol* **40**: 344–349.

Oleksy A, Opalinski L, Derewenda U, Derewenda ZS, Otlewski J. (2006). The molecular basis of RhoA specificity in the guanine nucleotide exchange factor PDZ-RhoGEF. *J Biol Chem* **281**: 32891–32897.

Olofsson B. (1999). Rho guanine dissociation inhibitors: pivotal molecules in cellular signalling. *Cell Signal* **11**: 545–554.

Ouhtit A, Gaur RL, Abd Elmageed ZY, Fernando A, Thouta R, Trappey AK *et al*. (2009). Towards understanding the mode of action of the multifaceted cell adhesion receptor CD146. *Biochim Biophys Acta* **1795**: 130–136.

Raucher D, Stauffer T, Chen W, Shen K, Guo S, York JD *et al*. (2000). Phosphatidylinositol 4,5-bisphosphate functions as a second messenger that regulates cytoskeleton–plasma membrane adhesion. *Cell* **100**: 221–228.

Ridley AJ. (2006). Rho GTPases and actin dynamics in membrane protrusions and vesicle trafficking. *Trends Cell Biol* **16**: 522–529.

Saci A, Carpenter C. (2005). RhoA GTPase regulates B cell receptor signaling. *Mol Cell* **17**: 205–214.

Shibasaki Y, Ishihara H, Kizuki N, Asano T, Oka Y, Yazaki Y. (1997). Massive actin polymerization induced by phosphatidylinositol-4-phosphate 5-kinase *in vivo*. *J Cell Biol* **272**: 7578–7581.

Shih IM, Elder DE, Speicher D, Johnson JP, Herlyn M. (1994). Isolation and functional characterization of the A32 melanoma-associated antigen. *Cancer Res* **54**: 2514–2520.

Shih IM, Speicher D, Hsu MY, Levine E, Herlyn M. (1997). Melanoma cell–cell interactions are mediated through heterophilic Mel-CAM/ligand adhesion. *Cancer Res* **57**: 3835–3840.

Takahashi K, Sasaki T, Mammoto A, Takaishi K, Kameyama T, Tsukita S *et al*. (1997). Direct interaction of the Rho GDP dissociation inhibitor with ezrin/radixin/moesin initiates the activation of the Rho small G protein. *J Biol Chem* **272**: 23371–23375.

Tsukita S, Yonemura S. (1999). Cortical actin organization: lessons from ERM (ezrin/radixin/moesin) proteins. *J Biol Chem* **274**: 34507–34510.

Witze ES, Litman ES, Argast GM, Moon RT, Ahn NG. (2008). Wnt5a control of cell polarity and directional movement by polarized redistribution of adhesion receptors. *Science (New York, NY)* **320**: 365–369.

Worthylake RA, Burridge K. (2003). RhoA and ROCK promote migration by limiting membrane protrusions. *J Biol Chem* **278**: 13578–13584.

Wu GJ, Peng Q, Fu P, Wang SW, Chiang CF, Dillehay DL *et al*. (2004). Ectopical expression of human MUC18 increases metastasis of human prostate cancer cells. *Gene* **327**: 201–213.

Wu GJ, Wu MW, Wang SW, Liu Z, Qu P, Peng Q *et al*. (2001). Isolation and characterization of the major form of human MUC18 cDNA gene and correlation of MUC18 over-expression in prostate cancer cell lines and tissues with malignant progression. *Gene* **279**: 17–31.

Xie S, Luca M, Huang S, Gutman M, Reich R, Johnson JP *et al*. (1997). Expression of MCAM/MUC18 by human melanoma cells leads to increased tumor growth and metastasis. *Cancer Res* **57**: 2295–2303.

Yan X, Lin Y, Yang D, Shen Y, Yuan M, Zhang Z *et al*. (2003). A novel anti-CD146 monoclonal antibody, AA98, inhibits angiogenesis and tumor growth. *Blood* **102**: 184–191.

Yang NY, Pasquale EB, Owen LB, Ethell IM. (2006). The EphB4 receptor-tyrosine kinase promotes the migration of melanoma cells through Rho-mediated actin cytoskeleton reorganization. *J Biol Chem* **281**: 32574–32586.

Zheng C, Qiu Y, Zeng Q, Zhang Y, Lu D, Yang D *et al*. (2009). Endothelial CD146 is required for *in vitro* tumor-induced angiogenesis: the role of a disulfide bond in signaling and dimerization. *Int J Biochem Cell Biol* **41**: 2163–2172.

Supplementary Information accompanies the paper on the Oncogene website (http://www.nature.com/onc)